Numerical Simulation of Mixed Mode Crack of Concrete: A Case Study Based on Experiment of Double Notched Specimen

Author: Quanxin Jiang
Supervisor: Max A.N. Hendriks
Yuguang Yang

Contents

1. Introduction

Concrete is the most widely used material in current construction field with more than 10 billion tons' consumption per year. Its applications vary from building, bridge, to roads and railways. Normally, concrete is considered to carry compression force because its tensile strength is much lower than compressive strength. In practice it is often inevitable to induce tension in concrete components and reinforcements are applied to ensure safety. Under such situations, cracks will initiate and propagate.

The computational modelling of crack is based on fracture mechanism, where crack can be classified into three basic modes: opening mode (Mode I), shear mode (Mode II), tearing mode (Mode III). [1] Mode I occurs due to normal load, while Mode II results from in-plane shear and Mode III caused by out-of-plane shear. With in-plane load, there is also a mixed mode of Mode I and Mode II, which is very common in real structures. However, the characteristic of mixed mode is more complex because of the combination of tension and shear.

The objective of this research is to find a proper nonlinear finite element approach to simulate mixed mode crack in concrete structures and give estimation on mesh size sensitivity of the simulation. The simulation is based on a case study which is described in the paper *Constitutive Mixed Mode Behavior of Cracks in Concrete* by Jacobsen [2]. The numerical simulation is performed with the software DIANA. Based on the difference of numerical results and experimental results, an estimation is made regarding to the simulation and the mesh size sensitivity. The study emphasizes on estimation of nonlinear finite element approach and from the view of engineers, with a focus on how engineers can simulate mixed mode crack with commercial software.

2. Experimental setup and results

In 2012, Jacobsen performed an experiment to establish an experimental basis for the mixed mode cracking. He used a double notched concrete specimen with a closed control loop. The biaxial testing machine is stiff enough to ensure a stable crack initiation and a controllable mixed mode opening. The experiments include mixed mode crack development with different initial Mode I opening and different mixed mode angles. This work is chosen as the case study of this research.

2.1 Geometry

The geometry of the double notched specimen is shown in Figure 1. The specimen has a length along y direction of 150mm, a width along x direction of 75mm and a height along z direction of 80mm. The notch is 55mm in length, 75mm in width and 4mm in height. The specimen is symmetric in three dimensions.

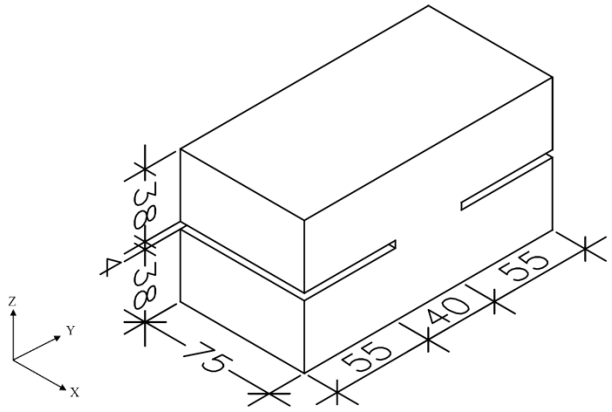

Figure 1: Geometry of the specimen

2.2 Material property

The specimen is of plain concrete. Concrete properties are given in Table 1.

Tensile strength	E	ν	Fracture Energy	Compressive strength	Compressive Fracture Energy	Aggregates
3.3N/mm^2	31Gpa	0.22	140N/m	41 N/mm^2	24600N/m	0.4-0.8mm

Table 1: Material Properties

2.3 Loading and boundary conditions

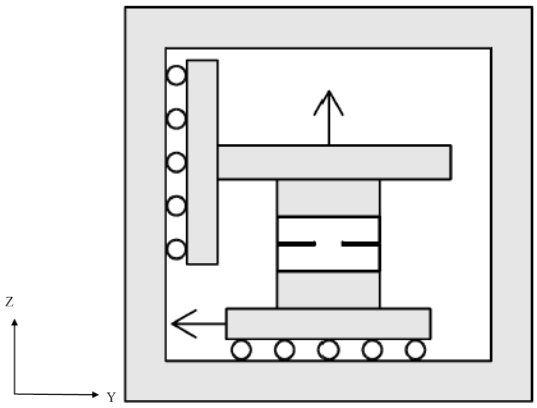

Figure 2: Specimen in testing machine

The applied stiff biaxial testing machine is capable of imposing both normal and shear displacement on the specimen. The specimen is glued to the machine on the top and bottom surface as shown in Figure 2. An orthogonal gauge is used to measure the opening and sliding components of the mixed mode displacement, and the measurements are used directly in the closed control loop. The testing machine imposes vertical displacement on the top surface of the specimen and shear displacement on the bottom surface of the specimen.

The loading process is under control in terms of relative displacement between the specimen part above and below the notch, namely Δu_s for relative shear displacement and Δu_n for relative normal displacement. Initially a crack is introduced between the notch by a pure Mode I opening and the crack is opened to a specified crack opening measured by the clip gauges. After the initiation of the crack the specimen can be

exposed to both Mode I and II opening introducing a mixed mode opening of the crack. The mixed mode opening angle is defined as the angle between the horizontal plane and the incremental relative displacement. The initial, vertical displacement velocity is 0.1μm/s, while the mixed mode opening pace is gradually increased to a final opening pace of 2.0μm/s. [2] The case study chooses experimental data with initial Mode I opening of 0.025mm with mixed mode angle of 40°, 45°, 50°, 55° and 60°.

2.4 Results

The experiment contains tests of Mode I crack and tests of mixed mode crack. The results of the uniaxial tensile test are shown in Figure 3. From the uniaxial test, material properties including tensile strength, Young's modulus and fracture energy are verified.

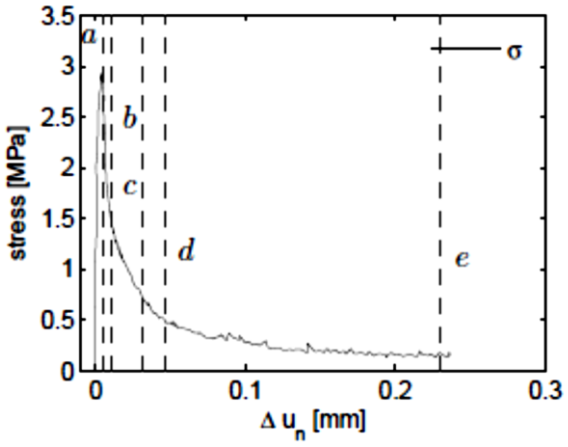

Figure 3: Stress-displacement result of uniaxial test [2]

The filtered results of mixed mode tests are presented in Figure 4. The figure shows the mixed mode behavior for five specimens with an initial opening of $\Delta u_n = 0.025$ mm followed by five different mixed mode angles ranging from 40° to 60°.

The shear stress level, shown together with the shear displacement in Figure 3 (a), increases for lowered mixed mode angle where the sliding starts to dominate. Figure 3 (b) combines the results from the three other plots and shows the shear stress, as function of the normal stress. Despite the few tests there is a clear tendency in the mixed mode behavior, where the results exhibit almost straight lines in the stress-plot in both loading and unloading before and after the peak, respectively. In Figure 3 (c) the initial opening of $(\Delta u_n, \Delta u_s) = (0.025,0)$ mm in each test is recognized and after the opening the five different mixed mode angles can be read from the figure. In Figure 3 (d) for the normal stress, there is a clear correlation between the level of compression and the size of the mixed mode angle. A lowered mixed mode angle is equal to a higher level of sliding and thereby intensified dilatational effects, which in the displacement controlled test results in more compression.

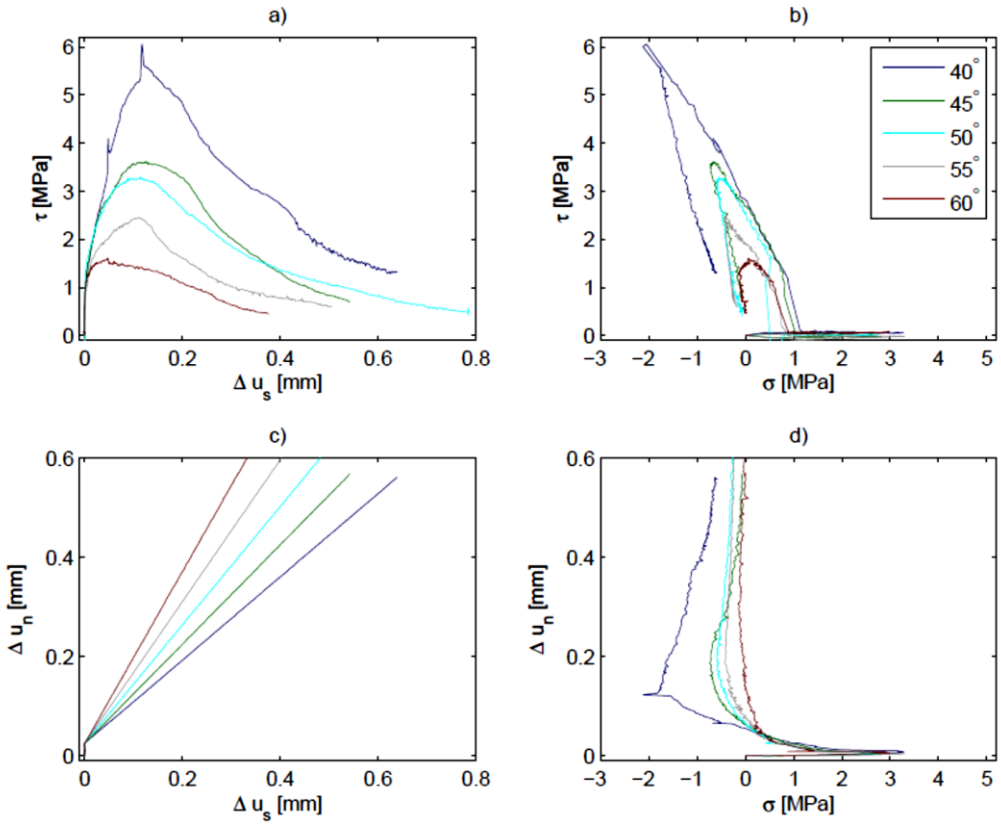

Figure 4: Stress and displacement curves of mixed mode test [2]

The fracture evolution at the surface is registered with the photogrammetric system Aramis. The pictures give an idea on how the primary crack between the notches develops and illustrates the amount of secondary fracture for varying mixed mode angles. For 40° an actual primary crack is not localized until the end of the experiment. The fracture development for 40° consists of two cracks propagating from each notch. Only at a late stage the two cracks coalesce into a primary crack between the notches. The crack between the notches is not completely straight and the crack pattern also includes some secondary cracking.

The secondary cracking seems less pronounced for 45° and the experiment ends with a distinct primary crack between the notches and minor secondary cracking primarily localized at the right notch. For 50° the crack is snapped directly at this transition and despite a clear, primary crack some secondary cracks tend to grow in crack planes inclined with respect to the ligament area. The final fracture development for loads returning to zero, where a clear fracture area is localized representing some secondary cracks and a distinct primary opening crack.

For 60° the final crack pattern consists of one primary crack between the notches and a second crack propagating parallel with the first one from the left notch towards the right notch. Even though the fractured area seems overwhelming, the extent perpendicular to the notch-line is in the range of the notch width (4 mm) and below the maximum aggregate size of 8 mm.

3. Finite element model

3.1 Material model and property

The concrete model is chosen as total strain based crack model with:

- Rotating crack orientation;
- 0.5mm, 1mm, 2mm crack bandwidth (the height of element in z direction);
- Vecchio & Collins 1993 (lower bound: 0) compression reduction model;

Note:

(1) The crack bandwidth is assumed equal to the value of element height (dimension in z direction), because the cracks mainly open in z direction.

(2) The effect of using fixed crack orientation model is also studied. As using rotating crack orientation gives a better simulation, it is chosen for the presentative model and mesh sensitivity study.

The mechanical properties are presented in Table 2.

Tensile strength	E	ν	Fracture Energy	Tensile curve	Compressive strength	Compressive Fracture Energy	Compression curve
3.3N/mm^2	31Gpa	0.22	70N/m	Exponential	41 N/mm^2	12300N/m	Parabolic

Table 2: Material properties of concrete model

Note:

Because the model is only half of the specimen, all prescribed displacements are reduced to a half due to the use of symmetry and antisymmetric. In the case, crack width is not intended to describe the real crack width in the specimen but stands for the average displacement difference in the normal direction of the crack. As the crack opening is mainly in z direction, crack width is assumed equal to Δu_n. When the prescribed displacement Δu_n is reduced to a half, the critical crack width should also be reduced. Figure 5 shows the reduction of critical crack width and as consequence the fracture energy is changed to approximately a half of the original one.

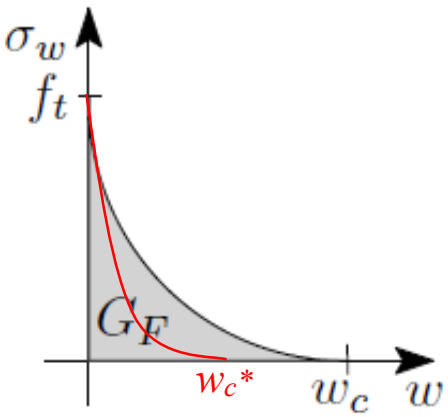

Figure 5: Tensile curve after crack initiated

3.2 Element type and finite element mesh

The 20-node brick element (CHX60) are used. The size of elements is presented in Table 3. The mesh is presented as Figure 6.

	Outside notched part	Notched part (representative model)	Notched part (coarse mesh)	Notched part (fine mesh)
x	7.5mm	4mm	4mm	4mm
y	7.5mm	3.75mm	3.75mm	3.75mm
z	9.5mm	1mm	2mm	0.5mm
Crack bandwidth	/	1mm	2mm	0.5mm

Table 3: Element size

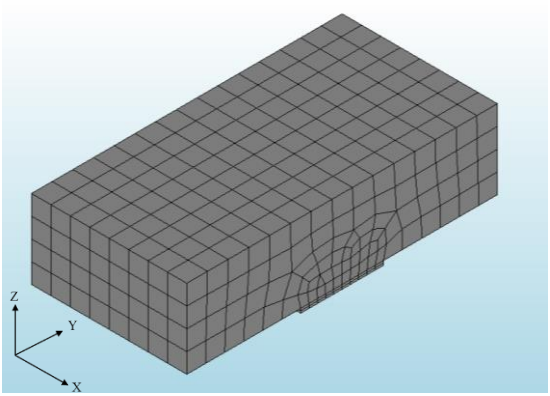

Figure 6: Mesh of the model

3.3 Boundary condition and loading

In the experiment, the top surface of the specimen was glued to testing machine and was applied with vertical displacement. In FE model, constrains in *x*, *y* and *z* directions were attached to the top surface and prescribed deformation in z direction was applied (Figure 7). Because only half of the specimen was modeled, the bottom surface in FE model represent the middle surface of the notched part. Interpretation of the condition of this surface is needed. In experiment, the middle surface of notched part was constrained by the other part of the specimen and was under a shear load due to the relative sliding movement between the two sides of the notch. In FE model, constrains in x, y and z directions were attached to the bottom surface and prescribed deformation in y direction was applied (Figure 8). Effect of Poisson ratio was neglected.

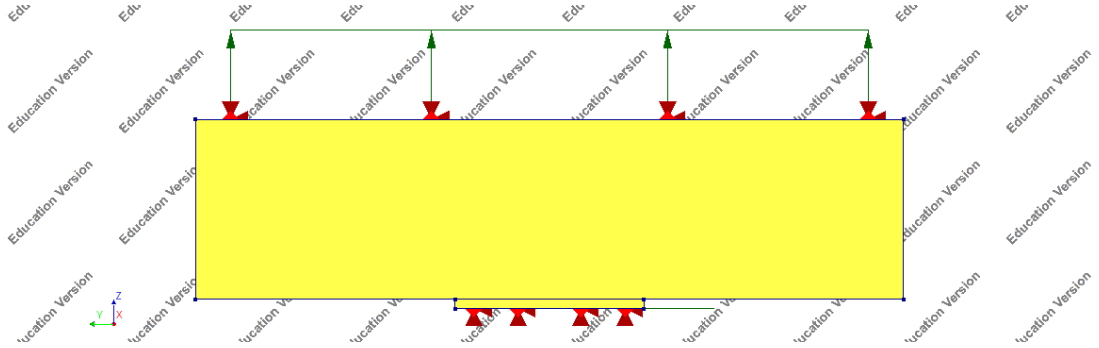

Figure 7: Side view of supports and loads

Note that due to symmetric geometry of the specimen and symmetry of the vertical displacement and antisymmetry of the shear displacement, the values of applied prescribed deformations in FE model were set as half of the values of displacement in

experiment.

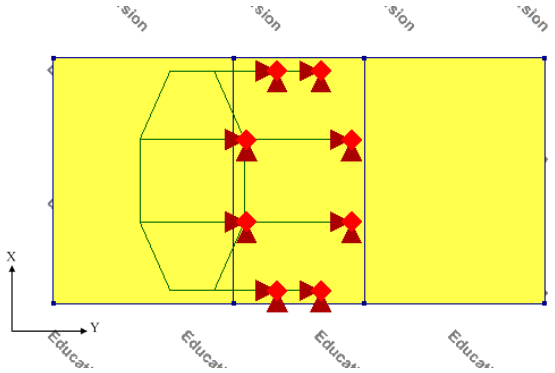

Figure 8: Bottom view of supports and loads

3.4 Load increments and convergence criteria

The analysis was divided into two phase: the first phase with only initial vertical prescribed displacement to initiate the Mode I crack opening; the second phase with a combination of vertical prescribed displacement and shear prescribed displacement to develop mixed mode crack opening with different mixed mode angles.

Initial vertical prescribed displacement (in z direction of 0.0125mm) was divided into 20 equal load steps. Regular Newton-Raphson scheme is used with maximum 20 iterations per step. Convergence tolerances equal to 1×10^{-3} and 1×10^{-2} were selected for energy and force norms, respectively. The iteration will stop if one of the criterions is met.

Combination of vertical prescribed displacement (in z direction of 0.2 mm) and shear prescribed displacement (in y direction varies from 0.1155mm to 0.24mm) was divided into 40 equal load steps. Regular Newton-Raphson scheme is used with maximum 40 iterations per step. Convergence tolerances equal to 1×10^{-3} and 1×10^{-2} were selected for energy and force norms, respectively. The iteration will stop if one of the criterions is met.

4. Nonlinear finite element analysis

4.1 Stress-displacement curve

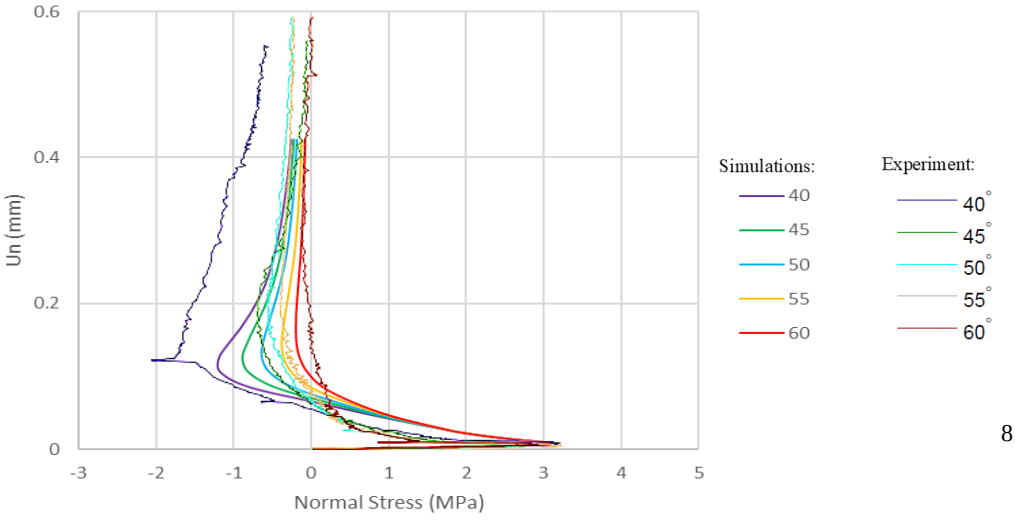

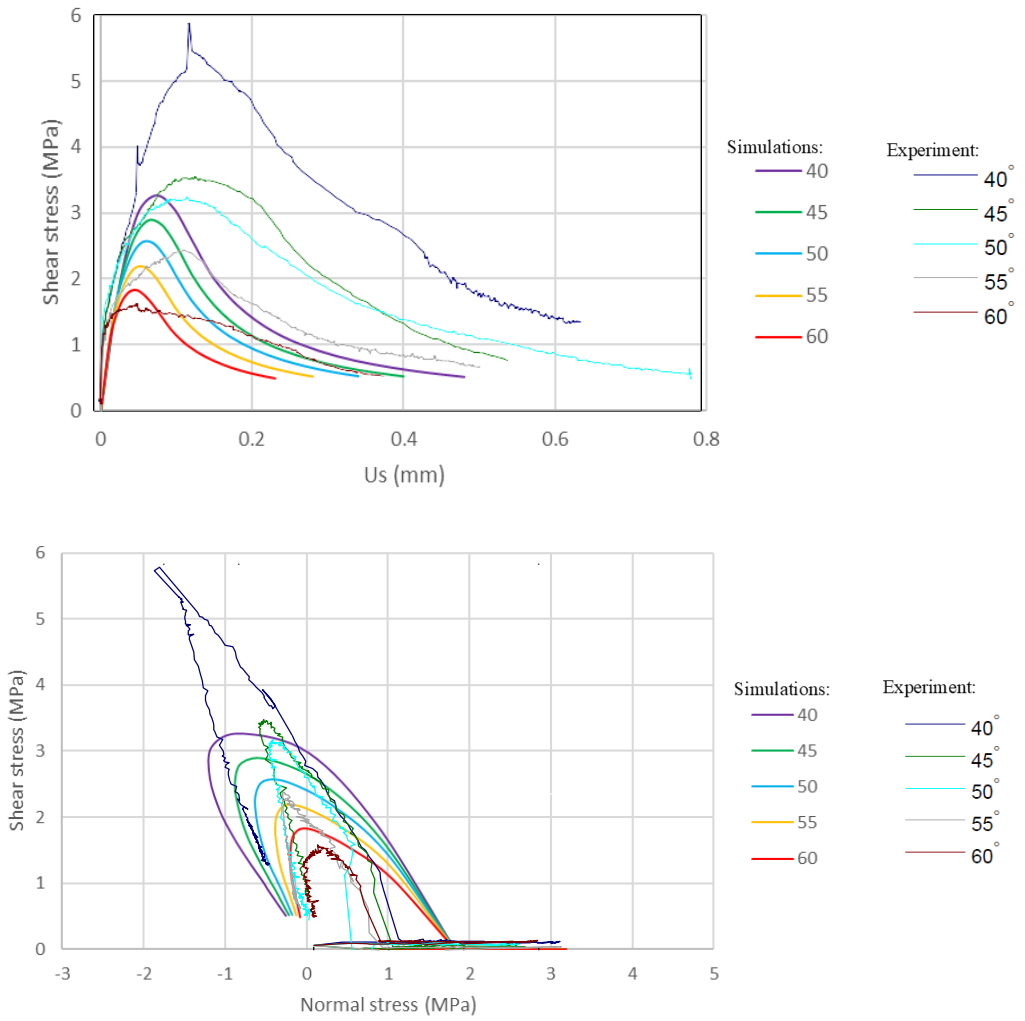

Figure 9: Stress and displacement curves of simulations and experiment

Figure 9 shows the model response of five different mixed mode angles with constant initial opening of 0.025mm. In Figure 9, simulated model response is compared with experiment. The smooth curves are simulation results and the rough curves are experiment results. The simulation is based on FE model with element height of h=1mm within the notched part. The initial Mode I opening stage is well recognized and the stress-displacement curves of mixed mode opening show right trends. However, the peak values of both normal stress and shear stress are not corresponding to experimental results.

For the mixed mode angle of 40°, the difference between simulated results and experiment is extremely apparent. The simulated normal stress is much lower during compressive stage and the shear stress also has a much lower peak value. Another difference is, the curves of shear stress have a quicker decrease after reaching the peak level. The comparison suggests that the simulation of mixed mode opening cannot fully initiate crushing between the crack surface and results in low level of friction. For other mixed mode angles, the difference between simulated results and experiment is less

significant. Figure 9 indicates that for large mixed mode angle (ie: 60°) the simulated results is close to experiment.

4.2 Convergence behavior

For Phase 1, where initial Mode I opening occurred, all the 20 load steps fulfill requirement of energy norm tolerance. For Phase 2, where mixed mode opening occurred, some load steps cannot achieve the convergence tolerance within maximum iterations. The convergence behavior of mixed mode angle 45° with element height 1mm is presented in Figure 10 as an example to illustrate the convergence behavior of Phase 2. After the first ten load steps, convergence was successfully reached based on energy criterion. The first ten load steps correspond to concrete behavior before losing traction, which refer to the curve before peak value in the figures. Even though convergence criterion is not satisfied in the first ten load steps, the relative variation is small enough (less than 2×10^{-3}) and can be expected to converge for a higher number of iteration chosen.

It can be noticed that the force norm was satisfied only for few load steps at the beginning of the Phase 1 analysis. In Phase 2 analysis, all load steps cannot reach convergence based on force criterion. Figure 11 shows the convergence behavior of Phase 2. The relatively large force variation could be one of the reason that the stress-displacement curve is not so desirable.

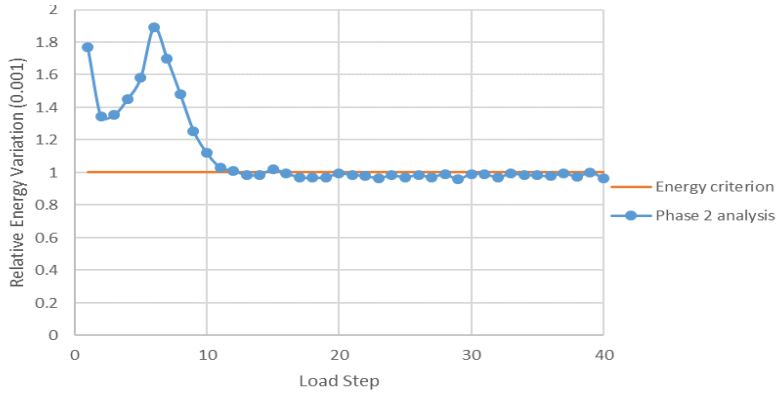

Figure 10: Convergence in terms of energy criterion

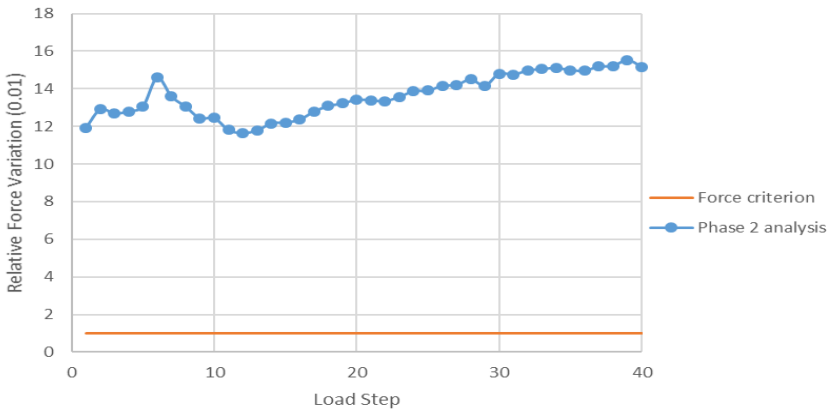

Figure 11: Convergence in terms of force criterion

4.3 Stress distribution

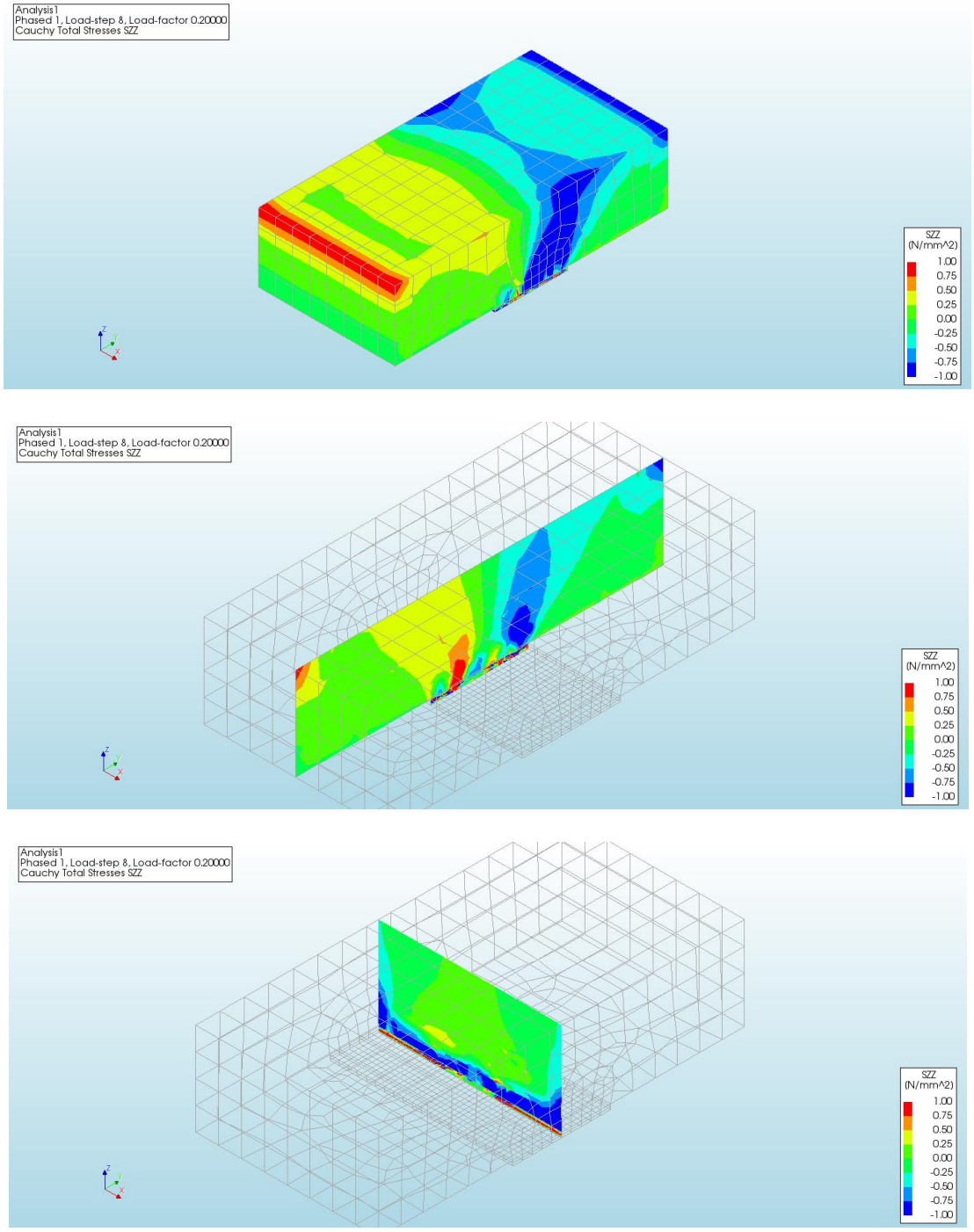

Figure 12: Stress distribution from isometric view

Figure 12 shows the distribution of σ_{zz} with mixed mode angel 45°, load factor 0.2 in Phase 2 (u_n= u_s =0.1mm) and element height h=1mm within notched part. The reason why chose load factor 0.2 is to present stress distribution when compressive stress is at peak level. From Figure 12, it is easy to determine the force flow in the macro-scale part (the part out of notch): tensile force flowed from the left upper corner (y=0 side) and compressive force flowed from the right upper corner (y=150 side). However, the force flow within notched part is complex. The slice of x=37.5mm and the slice of

y=75mm both suggests that the tensile force and compressive force “mix together” in notched part. In order to study what happened in the notched part, Figure 13 shows stress distribution of three slices: z=0mm (top plane), z=-1mm (middle plane) and z=-2mm (bottom plane).

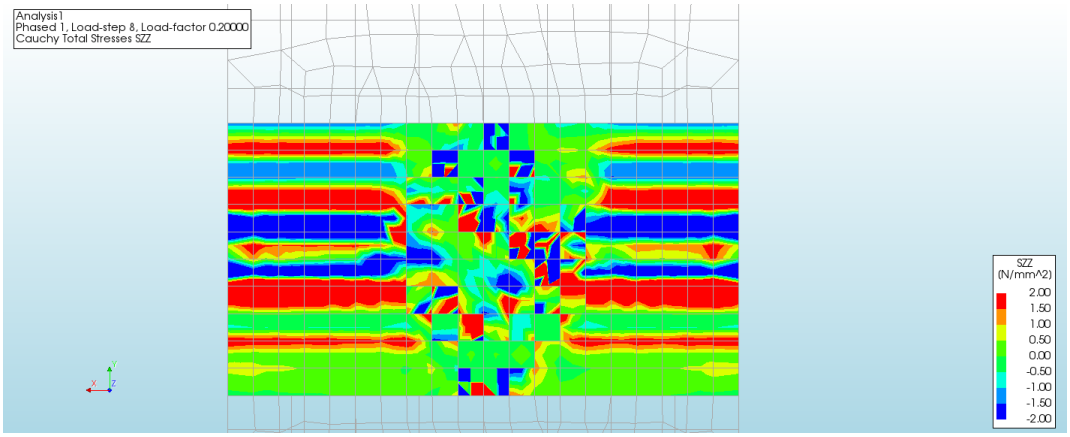

(a) Normal stress distribution at z=0mm (top plane)

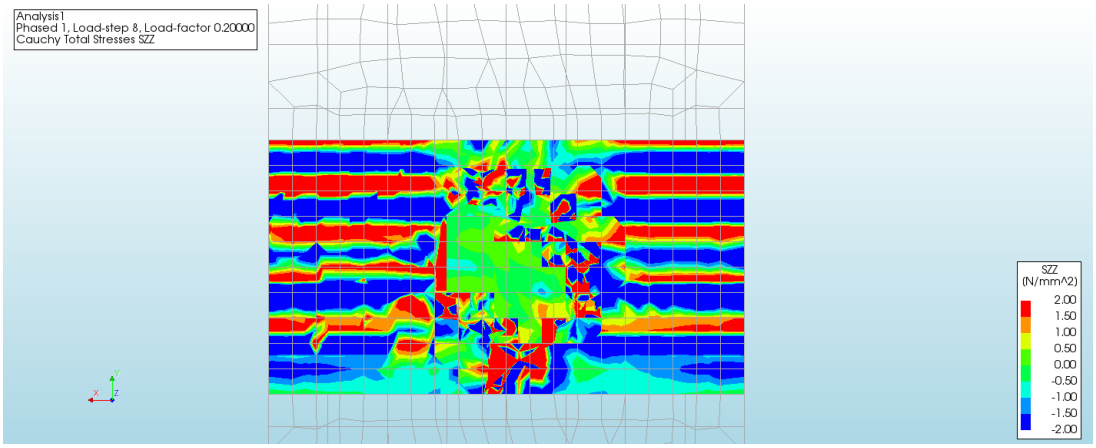

(b) Normal stress distribution at z=-1mm (middle plane)

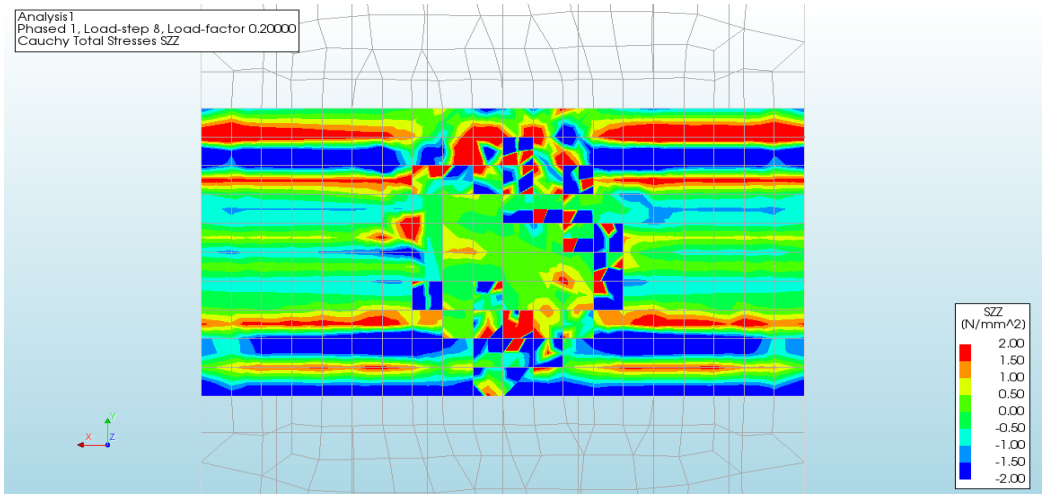

(c) Normal stress distribution at z=-2mm (bottom plane)

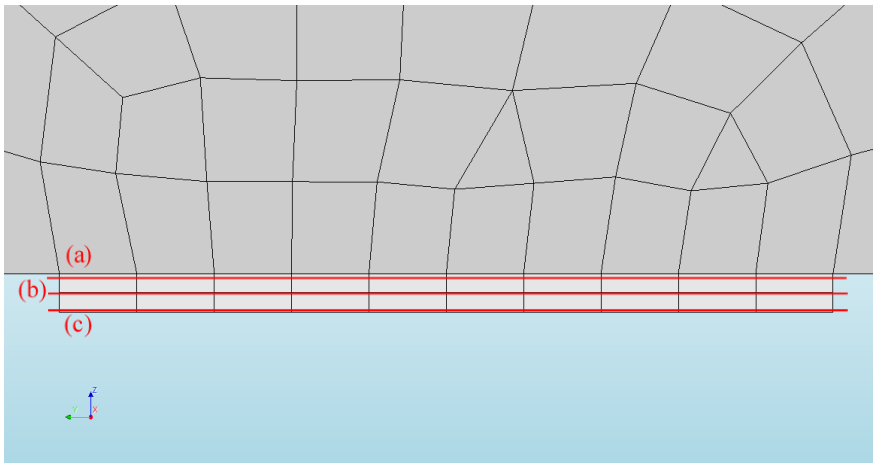

(d) Position of the three slices

Figure 13: Stress distribution of slices (a)z=0, (b)z=-1mm and (c)z=-2mm

From Figure 13, a "mixed" stress condition can be observed for all the three plane. The stress distribution suggests that part of the plane was in tension while part of the plane was in compression. If regard compressive part as where the crushing has been initiated, the stress distribution reflects that crushing process was partially initiated but not fully developed.

4.4 Crack width and crack strain

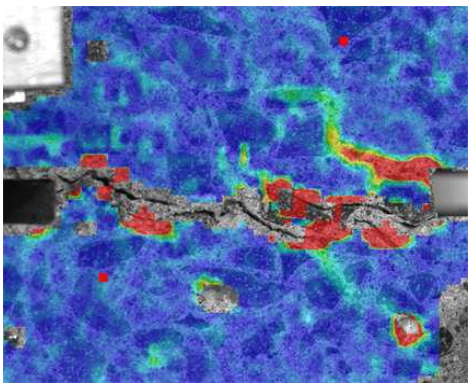

(a) Final crack pattern of 45°

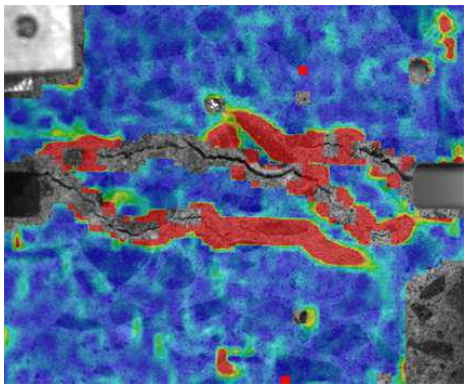

(b) Final crack pattern of 60°

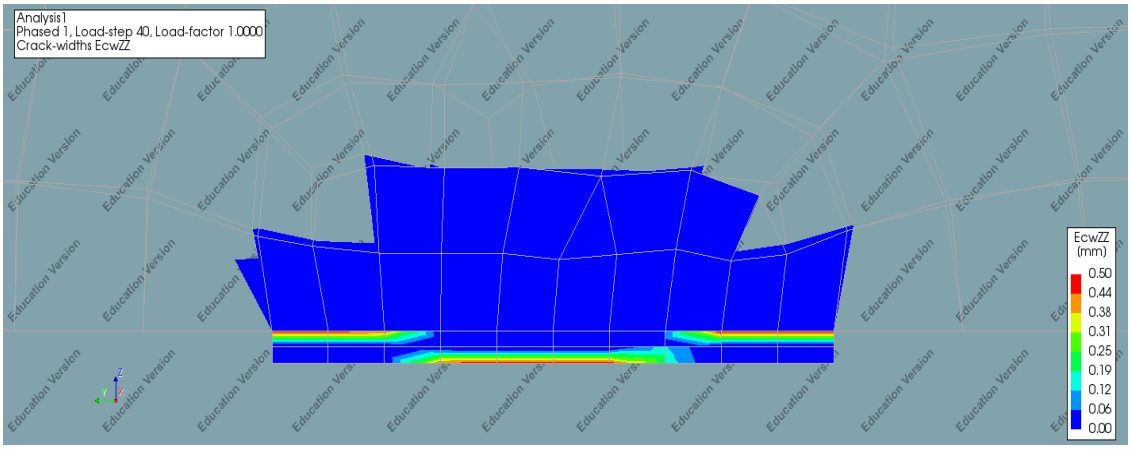

(c) Crack width of mixed mode angle 60°

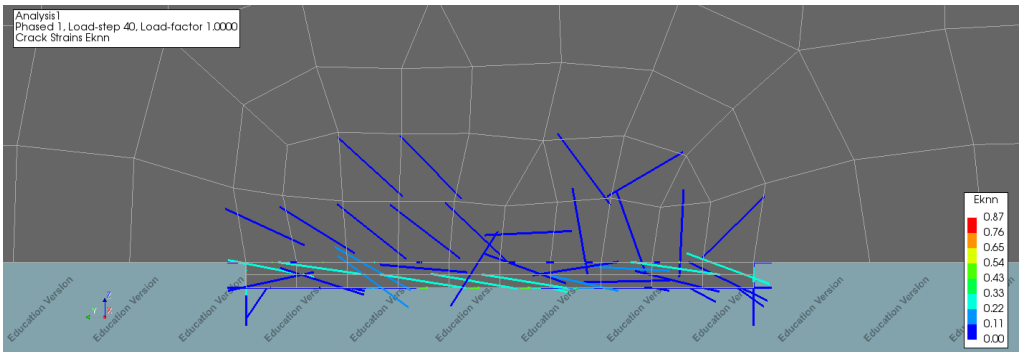

(d) Crack strain of mixed mode angle 60°

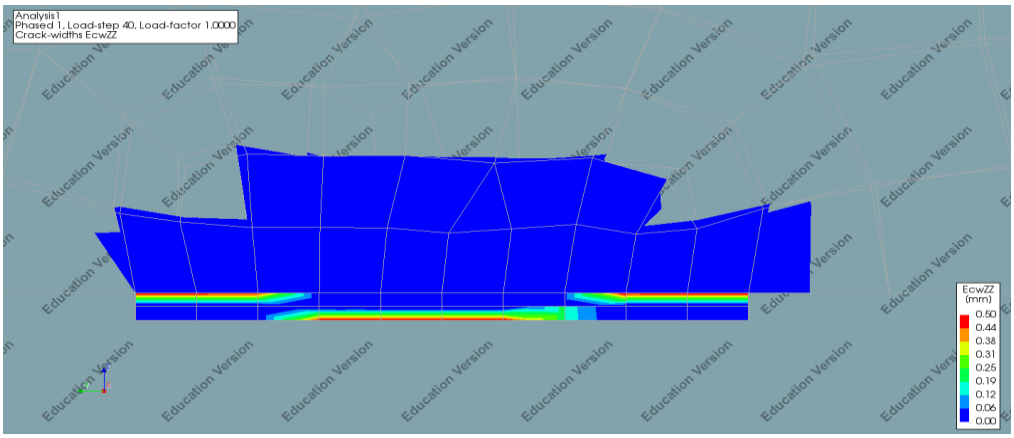

(e) Crack width of mixed mode angle 60°

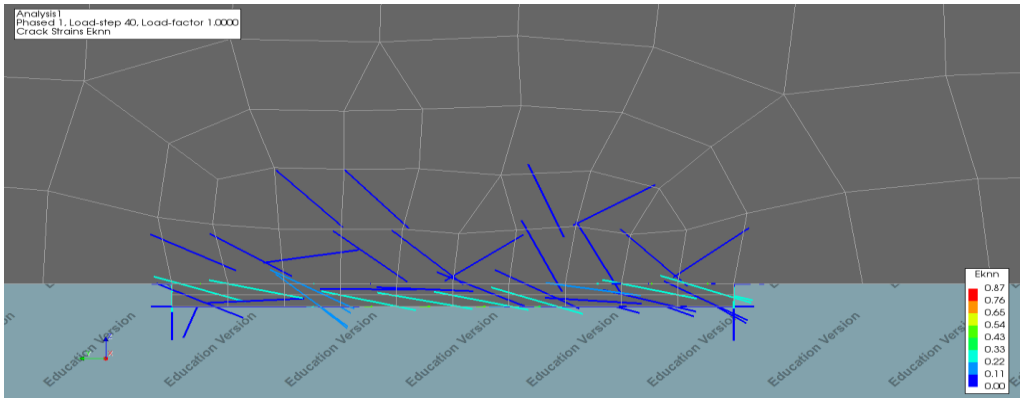

(f) Crack strain of mixed mode angle 60°

Figure 14: Comparison of crack pattern

Figure 14 shows real final crack pattern as well as the simulated crack width and crack strain of mixed mode angle 45° and 60°. Note that the simulation is only for the upper half part of the specimen. All interpretation of the simulated results should base on symmetry and antisymmetry. The crack pattern of simulation can be described as: the main crack initiated in initial stage keep developing in mixed mode load stage, while small cracks propagate to other part of the specimen. This basic pattern corresponds to experimental result. However, the primary crack in experiment has a different angle compared to the simulated one. In experiment, when mixed mode angle changed, the direction of primary crack also changed. In simulation, the direction of primary crack shows only slight difference when mixed mode angle changed. Obviously, the ideal

symmetric and homogenize model cannot perfectly simulate real crack propagation, but can provide information on possible development of the crack.

4.5 Mesh size sensitivity

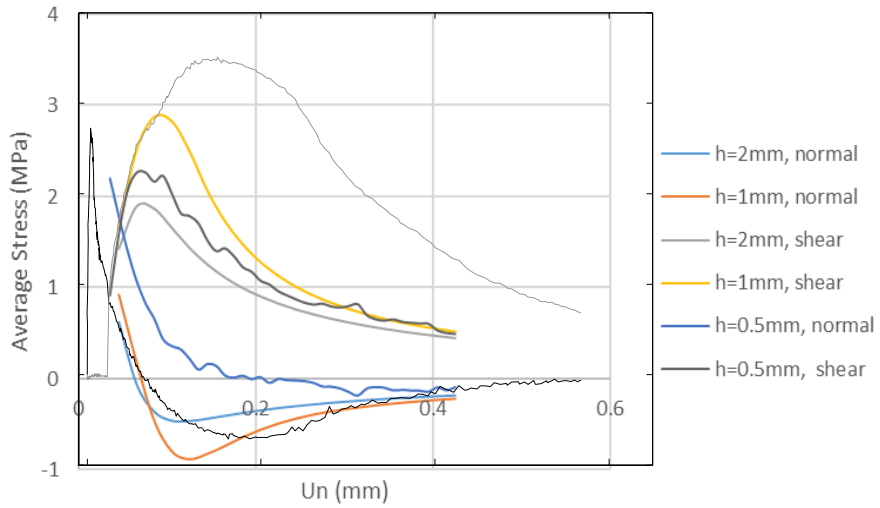

Figure 15: Stress-displacement relation of mixed mode angle 45

Figure 15 shows the stress-displacement relation of different simulations compared with the experiment. The black and grey rough curves are experimental curves and the simulation curves are only for Phase 2. It can be discovered that using element with 1mm height gives a much better simulation compared to using element with 2mm height or using element with 0.5mm height. When use element with 1mm height, the crushing process is relatively apparent (although the shear stress is still lower than experiment). If use element with 2 mm height, the trend of the curves is also correct but the peak value is even lower, which suggests the crushing process is less initiated. The element with 0.5mm height gave an unexpected result: not only the peak value is much lower, but the trend of normal stress curve is not correct. The decline of the normal stress curve is too slow and the compressive peak point is not presented.

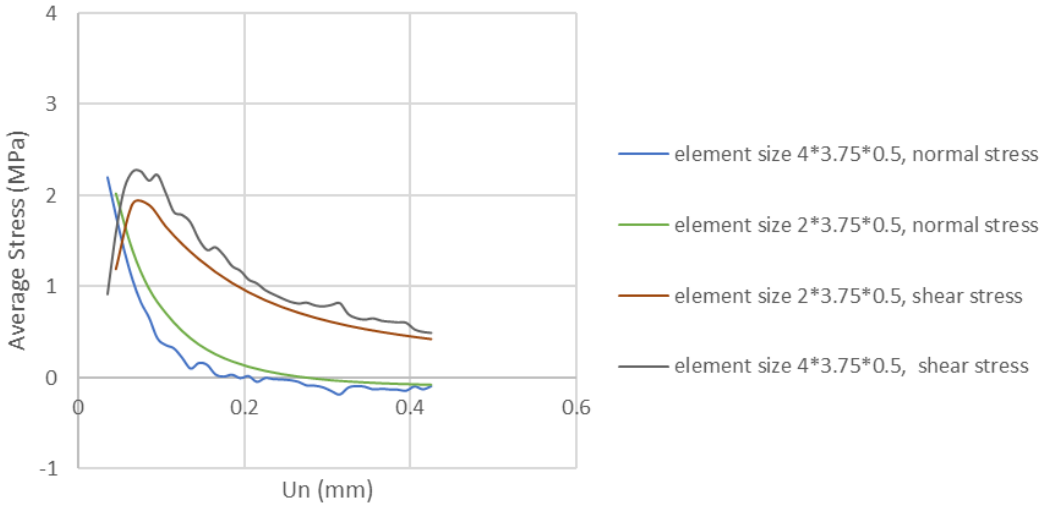

Figure 16: Stress-displacement relation of mixed mode angle 45

The main influence of mesh size is the height of elements within the notched part. Figure 16 and Figure 17 shows that the effect of the element size in the other two dimension is limited. And the size of elements outside notched part has little effect on results.

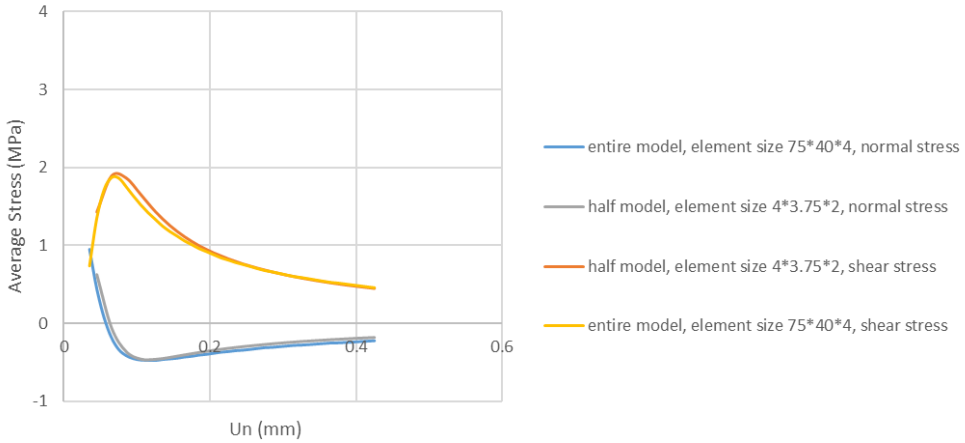

Figure 17: Stress-displacement relation of mixed mode angle 45

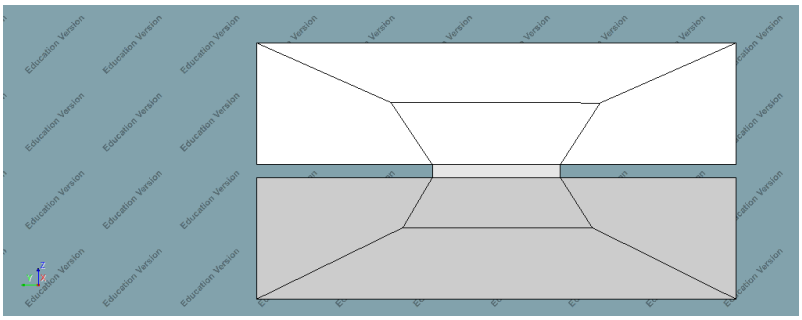

Figure 18: The entire model with element size of 75×40×4mm

4.6 Fixed orientation model

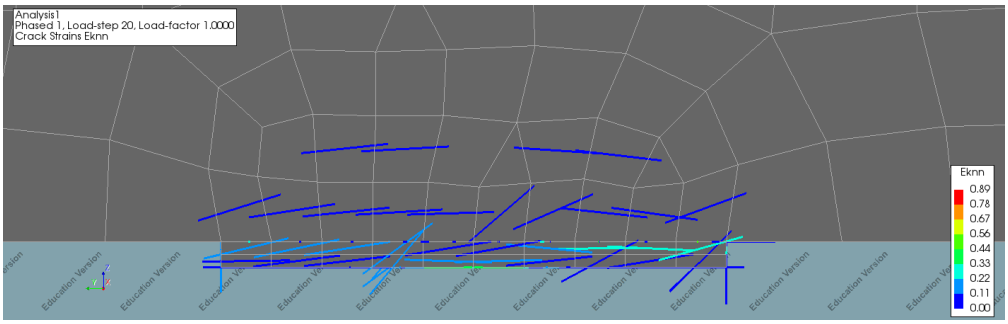

Figure 19: Crack strain of using fixed orientation model

Figure 19 shows the final crack strain of mixed model angle when use fixed orientation with damaged based shear model. It is obvious that the crack direction is not correct. The stress-displacement relation is also far away from experiment. If use "constant" shear model with retention factor 0.2, the direction of the crack seems more correct but the cracked area propagates beyond the notched part, as shown in Figure 20.

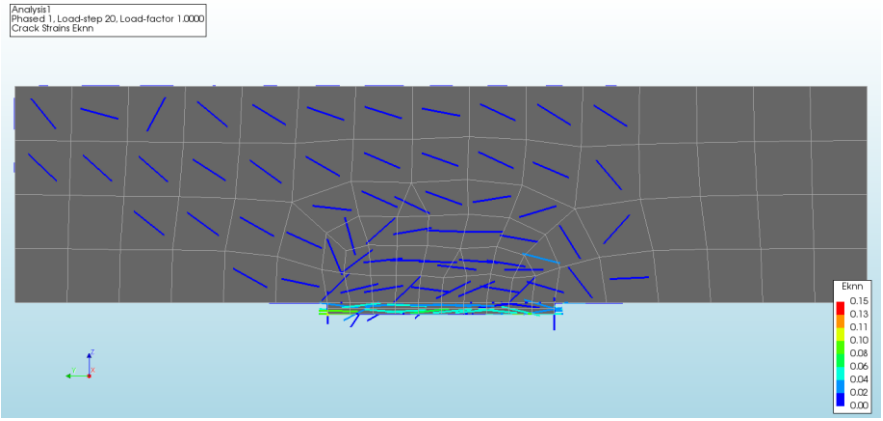

Figure 20: Crack strain of using fixed orientation model with retention factor

5. Discussion

5.1 Discussion about representative simulation results

The stress curves and stress distribution contour plots all suggest that the Mode I crack and mixed mode crack were recognized in the representative simulation. For mixed mode crack, the transition of average stress from tension to compression and the loss of traction were realized. Although the level of crushing was underestimated, the representative simulation managed to reflect the overall structural behavior of mixed mode crack. The underestimated crushing can be explained in three ways:

1) There are some load steps that did not satisfy convergence criterion and the force criterion has never been met. The convergence problem can cause inaccuracy of the results.

2) The model is of ideal symmetric and homogenize, which does not take influence of aggregates into consideration. However, aggregates play important role in crushing and shear behavior of concrete. It can lead to difference between ideal model and real structures.

3) Generation of the real crack surface is influenced by multiple factors which are not included in the simulation. The simulated crack surface is relatively smooth, which can lead to lack of friction and underestimated crushing.

5.2 Discussion about mesh sensitivity

The undesirable result of using mesh with h=0.5mm could be explained of very localized crack zone. The expected simulation should obtain a crack plane (or crack surface) where the crack width is relatively average distributed as the experiment did. Only if such a crack plane is obtained, average stress can be used to describe the behavior near the fracture zone. But when use mesh size h=0.5mm (four elements along half of the notched part), the crack was limited along the edge of bottom surface and top surface of the modeled notched part. (Figure 21 shows the crack width at the bottom surface for h=1mm and h=0.5mm.) Consequently, the simulation generated some localized crack zones with very large crack width and a crack plane with very small crack width. The failed generation of a crack plane with average distributed crack width has two effects: average stress cannot represent fracture zone behavior for both Mode I

crack and mixed mode crack; the model is no longer suitable to reflect real mixed mode crack behavior in 3D. Figure 22 shows the stress distribution at top surface for h=1mm and h=0.5mm. It is obvious that the crushing area was limited at the edge for h=0.5mm.

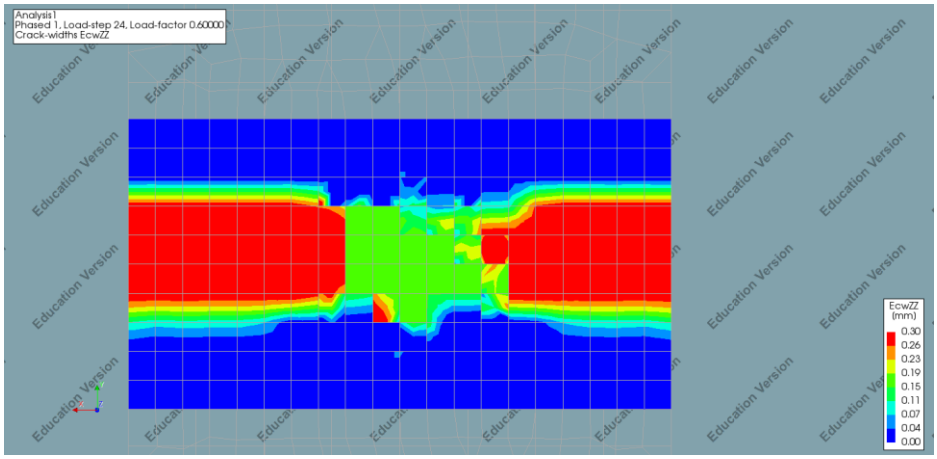

(a) Crack width at z=-2mm, element height=1mm

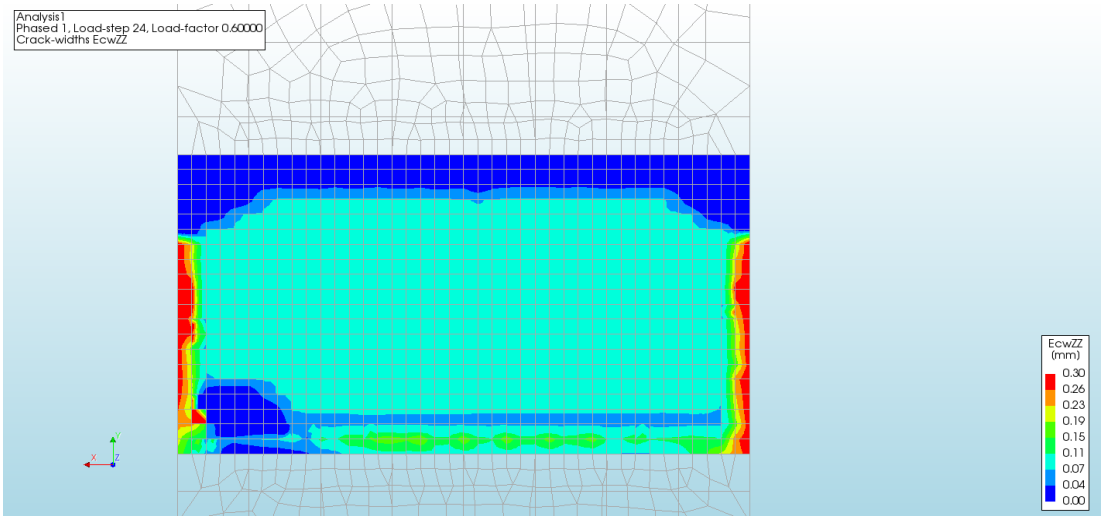

(b) Crack width at z=-2mm, element height=0.5 mm

Figure 21: Crack width at the bottom surface for h=1mm and h=0.5mm

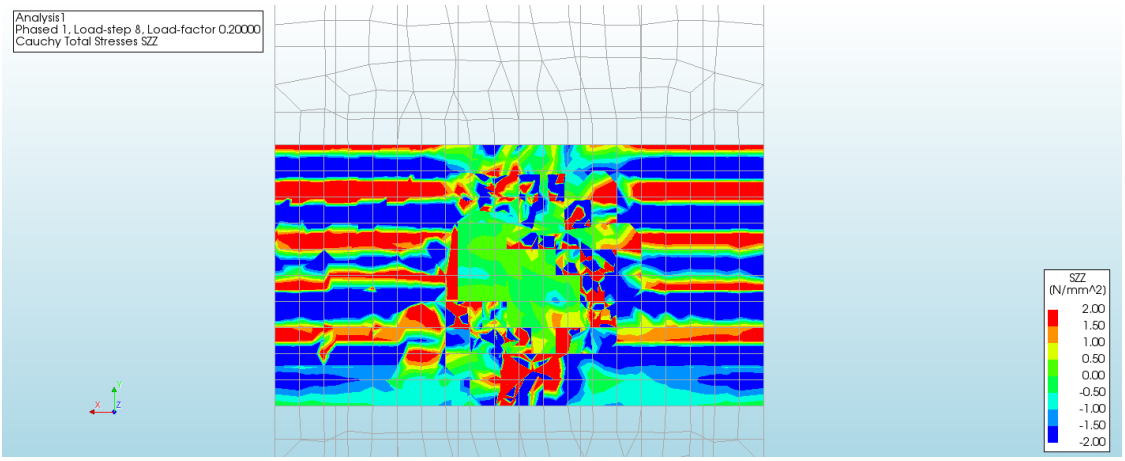

(a) Normal stress at z=0, element height=1mm

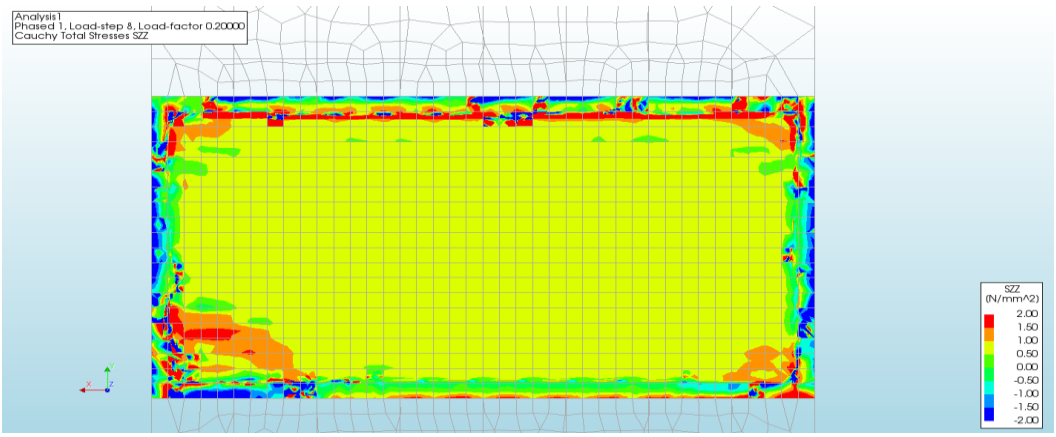

(b) Normal stress at z=0, element height=0.5mm

Figure 22: Stress distribution at top surface for h=1mm and h=0.5mm

The localization problem of using too small mesh size corresponds to the finding of Sluys and de Borst[3]. Sluys used 2D model to simulate crack of plain concrete specimen under pure tension. Using standard crack model and using G_f-type crack model both has results that localization zones are biased by the discretization and tend to propagate along mesh lines (Figure 23). The crack pattern in the 3D model of this research can be regarded as an extension of the 2D displacement patterns displayed in his article.

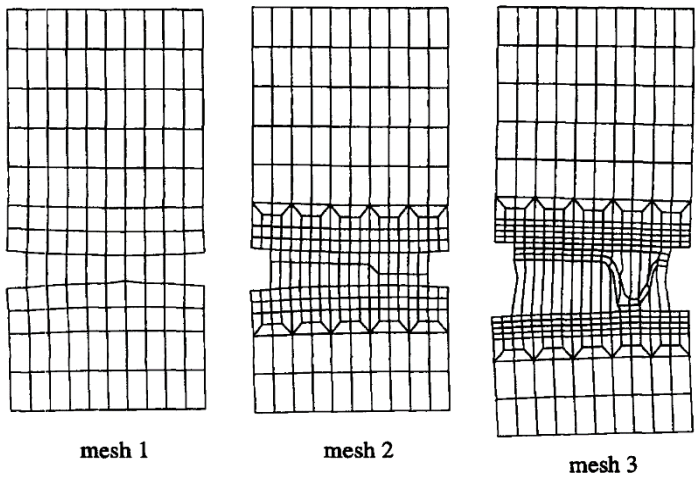

Figure 23: Displacement pattern [3]

Meanwhile, the less accurate result of too coarse element is expected. Using too coarse element causes a too wide crack bandwidth. The crack was averaged into a larger area compared to the actual cracked area. It failed to accurately describe the crack surface and failed to accurately reflect the structural response.

5.3 Discussion about crack orientation

The crack pattern and stress-displacement relation of using fixed crack orientation were undesirable. The crack direction suggests that the crack developed on the basis of Mode I opening, but did not change direction under mixed mode load. Such a result corresponds to the characteristic of fixed crack orientation model. In the fixed crack model, the principal axes of orthotropy are kept fixed during the post-cracking phase.

During Phase 1, the crack has been initiated with Mode I load and the principle stress and strain will be parallel to the load. In Phase 2, although load was changed to mixed mode, the crack direction would remain.

In terms of rotating crack orientation, the principal axes of orthotropy are not kept constant but rotate coaxially with the principal strains during crack propagation. It is possible for the crack to change direction during Phase 1 and Phase 2. The basic pattern corresponds to experimental result while the primary crack in experiment has a different angle compared to the simulated one. There are three possible cause for the difference:
1) As for the stress curves, it could be result of convergence problem.
2) The real propagation of crack is influenced by imperfections, aggregate distribution, load speed. Which are not included in simulation.
3) The cracked zones are biased by the discretization and tend to propagate along mesh lines.

6. Conclusion

In this research, simulation of small scale concrete specimen under mixed mode crack has been performed. The results qualitatively represent the characteristic of mixed mode crack behavior but quantitatively lack some accuracy. With a closer analysis, the simulation shows mesh dependence. Some concluding remarks can be driven to guide further study and application:

1) Due to ideal homogenize material model and difficulty to accurately describe the crack surface, crushing process is underestimate. To solve the problem, researchers are suggested to modify material model to include aggregates, imperfections and explore an effect way to describe the crack surface.
2) In the simulation, too fine or too coarse mesh both led to undesirable results. Researchers should be aware of that the crack is biased by the discretization and tend to propagate along mesh lines. Choosing improper mesh could lead to spurious crack pattern.
3) In the case of small-scale structure with multiple load phases, fixed crack orientation model failed to describe mixed mode crack. It is advised to use rotating crack orientation.
4) Convergence problem may occur in calculation. Researchers should choose small load steps during the early development of crack.

References

[1] M. B. Nooru-Mohamed (1992). Mixed-mode fracture of concrete: an experimental approach. Ph.D. thesis, Department of Civil Engineering, Delft University of Technology, Delft, Netherlands.
[2] J. S. Jacobsen (2012). Constitutive mixed mode behaviour of cracks in concrete: experimental investigations of material modelling. Ph.D. thesis, Department of Civil

Engineering, Technical University of Denmark, Lyngby, Denmark,
[3] L. J. Sluys and R. de Borst (1996). Failure in plain and reinforced concrete-an analysis of crack width and crack spacing. International Journal of Solids and Structures 33(20-22), 3257-3276.